# Comparative Study of Defect Reactivity in Graphene

**ARTICLE** *in* THE JOURNAL OF PHYSICAL CHEMISTRY C · SEPTEMBER 2013

Impact Factor: 4.77 · DOI: 10.1021/jp4061945



**2 AUTHORS**, INCLUDING:

Pablo A. Denis
University of the Republic, Uruguay
**104** PUBLICATIONS **1,563** CITATIONS

THE JOURNAL OF PHYSICAL CHEMISTRY C

Article

pubs.acs.org/JPCC

# Comparative Study of Defect Reactivity in Graphene

Pablo A. Denis* and Federico Iribarne

Computational Nanotechnology, DETEMA, Facultad de Química, UDELAR, CC 1157, 11800 Montevideo, Uruguay

**ABSTRACT:** We have applied dispersion corrected density functional theory to gauge the reactivity of the most common defects found in graphene. Specifically, we investigated single vacancies, 585 double vacancies, 555−777 reconstructed double vacancies, Stone−Wales defects, and hydrogenated zigzag and armchair edges. We found that the extent to which defects increase reactivity is strongly dependent on the (a) functional group to be attached and (b) number of functional groups attached. For the addition of one H, F, and phenyl groups to defective graphene, we found the following decreasing order of reactivity: single vacancy > hydrogenated zigzag edge > 585 double vacancy > 555−777 reconstructed double vacancy > Stone−Wales > hydrogenated armchair edge > perfect graphene. However, when two phenyl groups are attached, the Stone−Wales defect becomes more reactive than the 585 double vacancy and 555−777 reconstructed double vacancy. The largest increase of reactivity is observed for the functional groups whose binding energy onto perfect graphene is small. In contrast with recent experimental results, we determined that the reactivity of edges in comparison with perfect graphene is much higher than the reported value. When two groups are attached onto a 585, 555−777, or Stones−Wales defect, they prefer to be paired on the same CC bond on opposite sides of the sheet. However, for the single vacancy, this is not the observed behavior as the preferred addition sites are those carbon atoms that were previously bonded to the missing carbon.


## 1. INTRODUCTION

Structural defects play a key role in the chemistry and physics of graphene.[1] Their presence reduces the Young modulus and Poisson ratio,[2] induce magnetism,[3−5] and alter the chemical reactivity of graphene.[6−18] Defects are not purely theoretical speculations. They have been observed by aberration corrected high-resolution transmission electron microscopy. Some of the imaged defects include single vacancies,[19] 5−8−5 double vacancies,[19,20] 555−777 reconstructed double vacancy,[19] and Stone−Wales defects.[19]

The theoretical calculations that investigated the alteration of the chemical reactivity of graphene by defects showed that their presence enhances reactivity.[6−13] In effect, some functional groups can be attached only at defect sites.[6] For the azomethine ylide, addition of an isolated group to perfect graphene is endergonic, but exergonic on a Stone−Wales defect.[7] The ab initio study of the carboxylation of graphene by Al-Aqtash and Vasiliev[8] evidenced that point surface defects play a key role in the carboxylation of graphene. In the case of the single vacancy, it has been determined that this defect is so reactive that hydroxyl groups and water can be dissociatively adsorbed on it.[9,10] Another interesting finding that has been reported is that the presence of vacancies helps reduce the clustering of metal atoms and strongly attaches metal nanoparticles onto graphene.[11−15] In this vein, Lim and Wilcox[14] showed that a monovacancy plays a key role to ensure their stability on graphene and improve the catalytic activity toward $O_2$. Finally, the importance of defect sites in the interaction between microporous carbons (coals, gas shale) and $CO_2$ has been highlighted by Liu and Wilcox.[16−18] For example, they showed that, for a monovacancy, $CO_2$ physisorption is four times larger as compared with perfect graphene. In addition to this, the chemisorption of carbon dioxide at this defect site was very strong (1.72 eV).

All the studies about the reactivity of defective graphene demonstrated that chemical reactions are favored at defect sites. However, it is not clear which atoms of the defect sites are more reactive and what is more important, the ranking or reactivity of the defect sites. First-principles calculations have emerged as an essential tool to characterize nanomaterials.[19−34] Herein, we have employed density functional theory to study the reactivity of graphene containing the following structural defects: (a) single vacancies, (b) 555−777 reconstructed divacancies, (c) 585 divacancies, (d) Stone−Wales defects, and (e) zigzag and armchair edges. The results obtained provide a detailed comparison of the reactivity of structural defects and edges, answering important questions such as (i) which is more reactive: a zigzag edge or a single vancancy? (ii) Does the enhancement of reactivity depend on the functional groups attached? (iii) How reactive is a Stone−Wales defect? We expect that our findings may contribute to the tuning of the electronic properties of graphene by means of chemical functionalization,[22,23,28−31] help in the design of better $CO_2$ sequestration procedures,[16−18] and improve the mechanical properties of graphene−polymer nanocomposites, among many other applications of the functionalization of graphene.

## 2. METHODS

The selected methodology is similar to the one used to successfully study doped and functionalized gra-

**Received:** June 22, 2013
**Revised:** August 2, 2013
**Published:** August 10, 2013

   dx.doi.org/10.1021/jp4061945 | J. Phys. Chem. C 2013, 117, 19048−19055

phene.[5−7,23−25,28,29,31,32] Briefly, M06-L[35] and VDW-DF[36] calculations as implemented in Gaussian09[37] and SIESTA,[38,39] respectively, were carried out. The selected methodology has been employed in our previous work to study the magnetic properties of defective graphene.[5,34] For a detailed discussion, we refer the reader to these two works and references therein. The VDW-DF method was combined with the double-zeta basis set with polarization functions (DZP) and fixed the orbital confining cut-off to 0.01 Ry. The split norm used was 0.15. Results obtained with SIESTA can be prone to significant basis set superposition error (BSSE), even with relatively low degree of radial confinement.[6] For this reason, we used the counterpoise correction.[40] Relaxed structures were utilized to estimate the basis set superposition error (BSSE) and monomer deformation energies were taken into account. The interaction between ionic cores and valence electrons was described by the Troullier−Martins norm conserving pseudopotentials.[41] The Mesh cut-off was fixed to 200 Ry, which gave converged binding energies within 0.02 eV. For monolayer we used a 5 × 5 unit cell, even though some comparative calculations were performed with the 6 × 6 one. The results were similar for both unit cells. We optimized the lattice parameters along the *a* and *b* directions, but the *c* axis was maintained frozen at 20 Å. Unit cells were sampled using a Monkhorst−Pack *k*-point sampling scheme of 30 × 30 × 1 *k* points, which yielded converged results in all calculations. Geometry optimizations were pursued using the conjugate gradient algorithm until all residual forces were smaller than 0.01 eV/Å. The reactivity of graphene's edges was simulated employing zigzag and armchair nanoribbons. The unit cells were presented in our previous work about thiolated graphene.[6] In this case, we used a Monkhorst−Pack sampling of 500 × 1 × 1. Again, lattice parameters were optimized along the periodic direction and fixed to 25 Å in the nonperiodic ones. For the M06-L functional, the ultrafine grid and 6-31G*[42] basis set were used. We did not include basis set superposition error for the M06-L calculations since we have observed that the BSSE uncorrected M06-L/6-31G* results are similar to those obtained at the BSSE corrected M06-L/6-311G* level.[43]

## 3. RESULTS AND DISCUSSION

**3.1. Reactivity of the Single Vacancy.** The addition sites considered for this defect are presented in Figure 1. Although some of the seven positions are equivalent, 3 and 7 (numbering as in Figure 1), for example, we intended to be as comprehensive as possible and took into account only symmetry considerations for atom numbering. Binding energies (BE) are presented in Table 1. For the three radicals considered, the most reactive carbon atom is number 3 at all

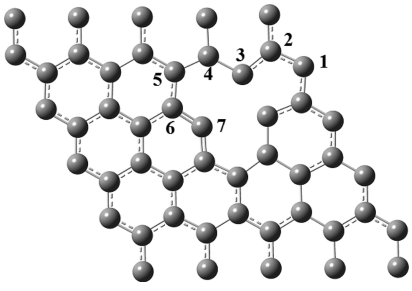


**Figure 1.** Graphene 5 × 5 with a single vacancy, functionalized with one group at different positions (1−7).

**Table 1. Binding Energies Determined for the Addition of Hydrogen, Fluorine, and Phenyl Radicals onto Perfect and Defective Graphene**

| | H | F | phenyl |
|---|---|---|---|
| | M06-L | M06-L | M06-L |
| G55 perfect | 16.7 | 30.2 | 8.8 |
| G55-Vac at 3 (956) | 99.0 | 103.8 | 88.1 |
| G55-Vac at 1 (665) | 41.8 | 50.3 | 33.8 |
| G55-Vac at 4 (966) | 39.3 | 38.8 | 24.2 |
| G55-Vac at 5 (966) | 34.3 | 48.6 | 30.2 |
| G55-Vac at 6 (966) | 23.6 | 31.5 | 17.8 |
| G55-Vac at 2 (966) | 29.0 | 32.6 | 18.4 |
| G55-SW-1 (775) | 37.6 | 55.0 | 32.6 |
| G55-SW-2 (765) | 33.9 | 44.2 | 27.8 |
| G55-SW-3 (665) | 29.5 | 40.5 | 23.8 |
| G55-SW-4 (766) | 25.5 | 36.9 | 16.9 |
| G55-SW-5 (766) | 25.3 | 38.9 | 18.3 |
| G55-555−777-2 (775) | 49.6 | 55.2 | 40.0 |
| G55−555−777−3 (765) | 38.0 | 43.9 | 28.8 |
| G55-555−777-5 (665) | 30.2 | 36.8 | 24.5 |
| G55-555−777-4 (766) | 28.6 | 38.3 | 19.9 |
| G55−555−777−1 (777) | 21.7 | 37.0 | 13.9 |
| G55-555−777-7 (665) | 26.8 | 29.8 | 21.6 |
| G55-585-3 (865) | 51.4 | 56.1 | 41.5 |
| G55−585−1 (566) | 41.1 | 42.1 | 34.9 |
| G55-585-2 (566) | 34.6 | 42.2 | 29.6 |
| G55-585−4 (866) | 31.9 | 40.2 | 22.3 |

levels of theory. When a functional group is attached onto this carbon atom, it is lifted out of the graphene plane by 1 Å, and the CC distance between the two carbon atoms of the pentagon is contracted by 0.08 Å. According to M06-L/6-31G*, the BE are 99.0, 103.8, and 88.1 kcal/mol, for H, F, and phenyl, respectively. As can be seen in Table 2, these BE are 5.9, 3.4, and 10 times larger, respectively, than the BE computed for the addition of the same radicals onto perfect graphene. The reason for such large spread of values is that the ratio $E_{\text{bind defective}}/E_{\text{bind perfect}}$ is strongly dependent on the BE onto perfect graphene. This quantity (BE) reaches the largest value for fluorine and the lowest for phenyl. A different way of comparing enhancement of the reactivity due to the vacancy is using the $E_{\text{bind defective}} - E_{\text{bind perfect}}$ difference.

The BE are increased by 82.3, 79.3, and 73.6 kcal/mol for H, phenyl, and F, respectively. Although fluorine has the largest BE on atom 3 of the vacancy, the increment is 10 kcal/mol smaller than that observed for hydrogen. Thus, we can expect that the presence of this defect increases BE by at least 70 kcal/mol. For the rest of the atoms belonging to the vacancy, the reactivity is much smaller as compared with carbon 3. In effect, addition onto carbon 1 has a BE that is more than 50% smaller than the most reactive site. The addition of these radicals onto the vacancy occurs barrierless, as indicated by the M06L/6-31G* calculations. Finally, we would like to note that although some atoms are equivalent, the BE computed are different because we reached solutions with different spin contamination.

That is the case of the addition of the aryl group to atoms 2 and 6. The BE for addition onto these sites are a bit different because the doublet wavefucntions have different spin contamination, $\langle S^2 \rangle$ = 0.77 and 0.85, respectively.

**3.2. Reactivity of the 585 Double Vacancy.** In this case, because of the high symmetry of the defect, only 4 carbon atoms are necessary to assess its reactivity. The structure is


dx.doi.org/10.1021/jp4061945 | J. Phys. Chem. C 2013, 117, 19048−19055

Table 2. Ratio of Binding Energies ($E_{bind}$) Determined for the Addition of Functional Groups to Perfect and Defective Graphene and Enhancement (kcal/mol) of Binding Energies onto Defect Sites with Respect to the Addition on Perfect Graphene

| | H | F | aryl | H | F | aryl |
|---|---|---|---|---|---|---|
| | M06-L | M06-L | M06-L | VDW-DF + BSSE | VDW-DF + BSSE | VDW-DF + BSSE |
| ratio = $E_{bind\ defective}/E_{bind\ perfect}$ | | | | | | |
| G55 perfect | 1 | 1 | 1 | 1 | 1 | 1 |
| G55-VAC at 965 | 5.93 | 3.44 | 10.0 | 4.37 | 2.53 | 7.61 |
| G55−585 at 865 | 3.08 | 1.85 | 4.72 | 2.45 | 1.49 | 3.76 |
| G55−555−777 at 775 | 2.97 | 1.83 | 4.54 | 2.41 | 1.49 | 3.66 |
| G55-SW at 775 | 2.25 | 1.82 | 3.71 | 1.96 | 1.38 | 3.16 |
| zigzag edge | | | | 2.91 | 1.84 | 5.07 |
| armchair edge | | | | 1.75 | 1.25 | 2.68 |
| enhancement = $E_{bind\ defective} - E_{bind\ perfect}$ | | | | | | |
| G55 perfect | 0.0 | 0.0 | 0.0 | 0.0 | 0.0 | 0 |
| G55-VAC at 965 | 82.3 | 73.6 | 79.3 | 78.2 | 65.7 | 75.3 |
| G55-585 at 865 | 34.7 | 25.8 | 32.7 | 33.6 | 21.1 | 31.4 |
| G55-555−777 at 775 | 32.9 | 25.0 | 31.2 | 32.7 | 20.9 | 30.3 |
| G55-SW at 775 | 20.9 | 24.8 | 23.8 | 22.3 | 16.4 | 24.6 |
| zigzag | | | | 44.3 | 35.9 | 46.4 |
| armchair | | | | 17.4 | 11.1 | 19.2 |

presented in Figure 2. Calculations point to atom 3 (numbering as in Figure 2) as the most reactive one. When one of the

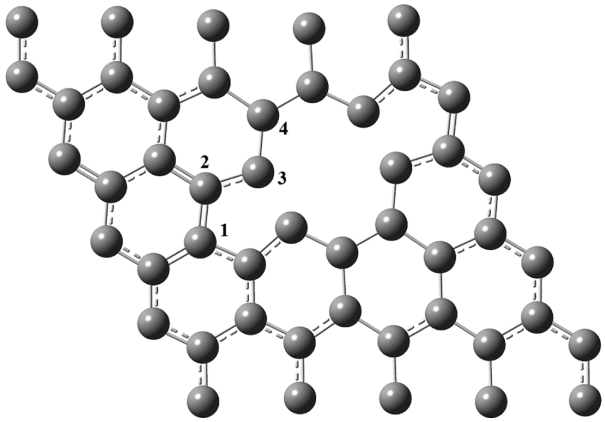


**Figure 2.** Graphene 5 × 5 with a 585 divacancy, functionalized with one group at different positions.

radicals considered is attached to atom 3, the curvature of the sheet becomes more evident. The lowest configuration of the 585 defective graphene ∪ graphene is curved. The planar defective sheet is 1.3 kcal/mol higher in energy. However, for the functionalized sheet, only the curved structure can be found. Functionalization decreases the CC distance of the opposite pentagon by 0.04 Å. The BE are 51.4, 56.1, and 41.5 kcal/mol for H, F, and phenyl, respectively. These BE are 34.7, 25.8, and 32.7 kcal/mol larger than the values computed for perfect graphene. As observed for the single vacancy, the most important increase is verified for hydrogen and the smallest for fluorine. In effect, for fluorine the site is less than two times more reactive than perfect graphene. However, the reactivity is 3.1 and 4.7 times larger for hydrogen and phenyl. In contrast with the results obtained for the single vacancy, we observe that reactivity of the defect is more uniform across the site: the energetic difference between the most reactive site and the less reactive one is less than 20 kcal/mol for the three cases considered.

**3.3. Reactivity of the 555−777 Reconstructed Double Vacancy.** This defect is slightly more stable than the 585 double vacancy and presents a structure that is very different because of the presence of three pentagons and three hexagons, as shown in Figure 3. In this case, the number of atoms

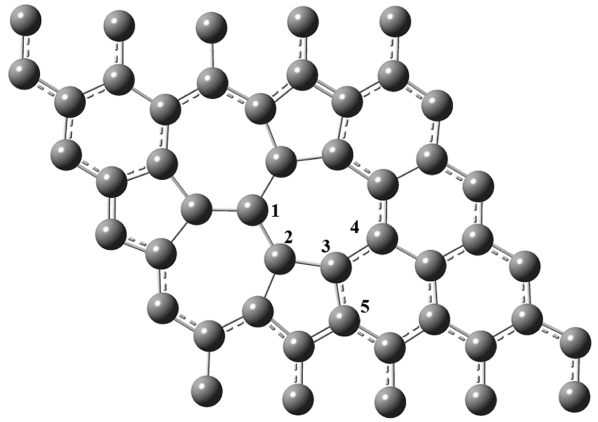


**Figure 3.** Graphene 5 × 5 with a 555−777 reconstructed divacancy, functionalized with one group at different positions (1−5).

necessary to map the reactivity is 5. The BE presented in Table 1 indicate that the most reactive carbon atom belongs to the junction of two heptagons and one pentagon. This functionalization induces small structural changes in the sheet since only the functionalized carbon atom is lifted by 0.2−0.3 Å. The BE for addition onto this atom are 49.6, 55.2, and 40.0 kcal/mol, for H, F, and phenyl, respectively. The least reactive carbon atom corresponds to the junction of the three heptagons, namely, carbon 1 (numbering as in Figure 3). This atom also shows the largest positive charge. Mulliken analysis suggested a value of +0.17. Although it is tempting to correlate charges with reactivity, this procedure is not adequate because the most negatively charged atom is carbon 5 (numbering as in Figure 3) with −0.12, and this atom is not the most reactive one. Carbon 2, the preferred atom for radical addition, has charge equal to 0.003.


dx.doi.org/10.1021/jp4061945 | J. Phys. Chem. C 2013, 117, 19048−19055

**3.4. Reactivity of the Stone–Wales Defect.** For this defect, we observe a similar trend to the one discussed for the 585 double vacancy: there is one atom, which has the largest reactivity but the rest of the atoms display a similar trait. In this sense, the difference between the largest and lowest BE is less than 14 kcal/mol. As expected, the most reactive carbon atom belongs to the junction of two pentagons (see Figure 4) and

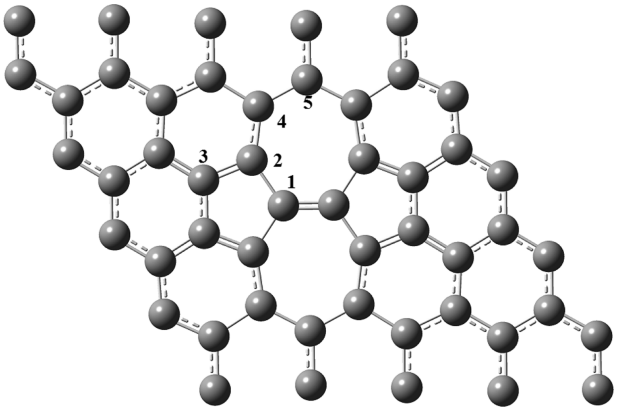


**Figure 4.** Graphene 5 × 5 with a Stone–Wales defect, functionalized with one group at different positions (1–5).

functionalization on this site strongly enhances the ripples of the sheet. In effect, the lowest carbon atom is 1.3 Å above the highest one. The BE for attachment onto this site are 37.6, 55.0, and 32.6 kcal/mol for H, F, and phenyl, respectively. Yet, there is an important difference between the Stone–Wales and the other defects assayed: the fluorine atom displays the largest increase of BE (24.8 kcal/mol) with respect to perfect graphene.

Also, the difference between the ratio of BE is not as important as compared with the other defects. For fluorine carbon 1 (numbering as in Figure 4) is 1.82 times more reactive whereas for hydrogen it is 2.25 times.

**3.5. Reactivity of Edges.** To analyze this defect, we have employed the VDW-DF method and the SIESTA program because it is easier to study the antiferromagnetic ground state of zigzag nanoribbons. The results are presented in Table 3. At the VDW-DF/DZP level, the zigzag edge is 2.91, 1.84, and 5.07 times more reactive for H, F, and phenyl, respectively, than perfect graphene. These values are a bit different than those reported by Sharma et al.[44] These authors attached 4-nitrobenzene diazonium tetrafluoroborate to edges and perfect graphene and found that the reactivity of the former is at least two times that of bulk graphene. Our calculations predicted a much larger difference (5.07 times) for the addition of phenyl radicals to perfect graphene and to zigzag edges. We note, however, that we have considered a zigzag edge that is terminated with an H atom. With a bare edge, the reactivity is expected to be even larger. The armchair edge is more chemically inert but even in this case the reactivity of the edge is 2.68 times larger than perfect graphene. The addition on the armchair edge increases BE by 17.4, 11.1, and 19.2 kcal/mol, for H, F, and phenyl, respectively. Again, using unsaturated armchair edges is expected to yield higher reactivity. Therefore, notwithstanding which type of edge was assayed, the reactivity of these sites in comparison with the perfect sheet is larger than the value suggested experimentally.[44]

**3.6. Ranking of Defects Reactivity.** Once the reactivity of all atoms belonging to the defect has been studied in detail, we are in position of comparing the reactivity of defects. All methodologies employed suggest the same order of decreasing reactivity: single vancancy > zigzag edge >585 > 555–777 > Stone–Wales > armchair edge. However, the extent of reactivity increase is not similar for different functional groups. Inspection of the results listed in Table 2 indicates that the smaller the BE of the functional group onto perfect graphene, the larger the enhancement of reactivity if the quotient $E_{\text{bind defective}}/E_{\text{bind perfect}}$ is considered. However, when the bonding between graphene and the functional group is strong, the reactivity of the defects is similar, except for the single vacancy. Such is the case of fluorine, for which the 585, 555–777, and Stone–Wales defect augment the BE by 25–26 kcal/mol. Finally, regarding the reactivity of edges, the hydrogenated zigzag edge is more reactive than all defects considered except for the single vacancy. The opposite situation was found for the saturated armchair edge, which is less reactive than all the other defects assayed.

**3.7. Cooperative Addition of Radicals onto Defects.** In previous works, we have reported that when free radicals such as H,[24] SH,[6] NH,[31] and organic functional groups such as benzynes[45] and azomethine ylides[46] are agglomerated onto perfect graphene, the BE are dramatically increased. For this reason, we studied here the effect of attaching two aryl radicals onto the single vacancy, 585 double vacancy, 555–777 reconstructed double vacancy, and the Stone–Wales defect. To attach the radicals, we have applied the following the rule: the first group is positioned on the most reactive carbon atom of the defect. The second is attached to the rest of the carbon atoms that belong to the defect. We have taken into account the double-sided addition as well as singlet and triplet ground states of the wave function. The numbering schemes are depicted in Figures 5–8 for the single vacancy, 585 double vacancy, 555–777 reconstructed double vacancy, and the Stone–Wales defect, respectively.

The BE are listed in Tables 4 and 5. For 585, 555–777, and Stone–Wales defects, a similar behavior is verified, the second

**Table 3. Binding Energies Determined for the Addition of Functional Groups to Perfect and Defective Graphene**

| | H | H | H | F | F | aryl | aryl |
|---|---|---|---|---|---|---|---|
| | M06-L | VDW-DF | VDW-DF + BSSE | M06-L | VDW-DF | M06-L | VDW-DF + BSSE |
| G55 perfect | 16.7 | 25.6 | 23.2 | 30.2 | 42.9 | 8.8 | 11.4 |
| G55-VAC at 3 (956) | 99.0 | 103.9 | 101.4 | 103.8 | 108.6 | 88.1 | 86.7 |
| G55-SW-1 (775) | 37.6 | 47.9 | 45.5 | 55.0 | 59.3 | 32.6 | 36.0 |
| G55-555–777-2 (775) | 49.6 | 58.4 | 55.9 | 55.2 | 63.8 | 40.0 | 41.7 |
| G55-585-3 (865) | 51.4 | 59.4 | 56.8 | 56.1 | 64.0 | 41.5 | 42.8 |
| zigzag edge | | | 67.5 | | 78.8 | | 57.8 |
| armchair edge | | | 40.6 | | 54.0 | | 30.6 |


dx.doi.org/10.1021/jp4061945 | J. Phys. Chem. C 2013, 117, 19048–19055

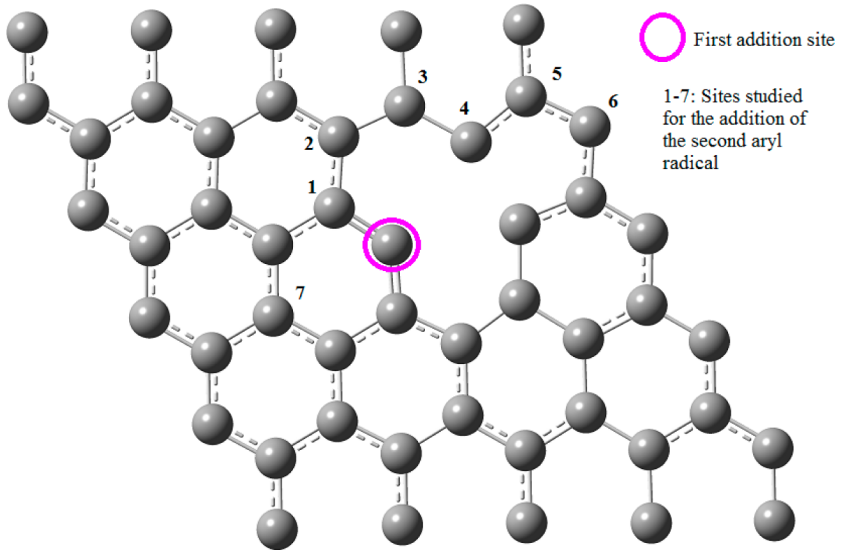


**Figure 5.** Addition sites studied for the addition of two aryl radicals onto monovacancy defective 5 × 5 graphene. Corresponding binding energies are presented in Table 4.

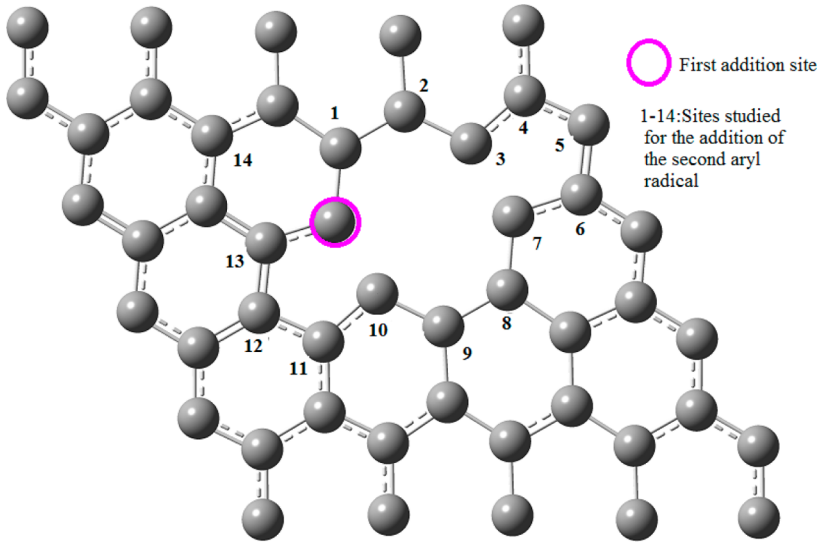


**Figure 6.** Addition sites studied for the addition two 2 aryl radicals onto 585 defective 5 × 5 graphene. Corresponding binding energies are presented in Table 5.

phenyl radical prefers to be attached onto a carbon atom that is bonded to the first phenyl group. The addition is performed on opposite sides of the sheet because of the size of the functional group. This addition pattern resembles the addition of H[22] and SH[6] radicals onto perfect graphene. Regarding the increase of reactivity obtained for pairing the phenyl radicals, the BE per aryl group are larger than those corresponding to the addition of one phenyl group to the defect. The most dramatic increase is noticed for the Stones−Wales defect as the BE per aryl group obtained for the attachment of two phenyl groups onto the CC bond that connects two pentagons is 52.2 kcal/mol. This value is 20 kcal/mol larger than the BE for the addition of one phenyl group onto Stone−Wales defective graphene. Also, it is 7.8 and 3.5 kcal/mol higher than the BE computed for the addition of two aryl radicals onto the 585 and 555−777 defects. Thus, for the addition of two aryl radicals, the Stone−Wales defect is more reactive than the 585 and 555−777 defects. In line with the results obtained for the single addition, the 585 defect is slightly more reactive than the 555−777. For the Stone-Wales, 585 and 555−777 defects, we can appreciate a preference for the singlet ground states. There is one difference between the single and double additions onto these three defects: the pairing of radicals produces a great spread of the computed BE, and thus, there is a strong preference for the addition on a nearby carbon atom. For the Stone−Wales defect, there is one carbon atom nearby that is preferred. However, for the 585 and 555−777 defects, there are two and three different types or nearby carbons, respectively. Finally, it has to be said that, for the 585 and 555−777 defects, there are one and two carbon atoms with high reactivity, but they are not directly bonded to the carbon atom bearing the first aryl radical. For the 585 defect, these atoms correspond to the two atoms on the opposite pentagon as shown in Figure 6. In the case of the 555−777 defect, the reactive atom is number five, and it has a structure similar to that of the carbon atom bearing the first phenyl group, i.e., it is located at the junction of two heptagons


dx.doi.org/10.1021/jp4061945 | J. Phys. Chem. C 2013, 117, 19048−19055

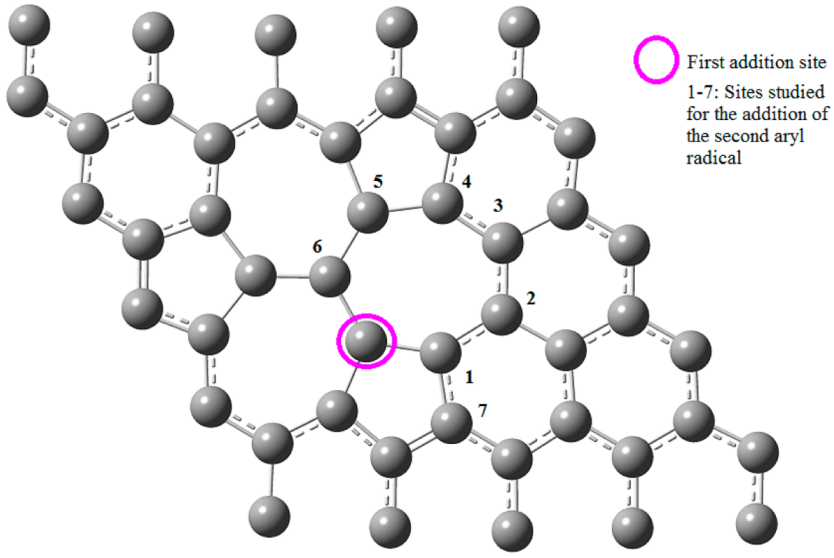


**Figure 7.** Addition sites studied for the addition of two aryl radicals onto 555−777 5 × 5 graphene. Corresponding binding energies are presented in Table 4.

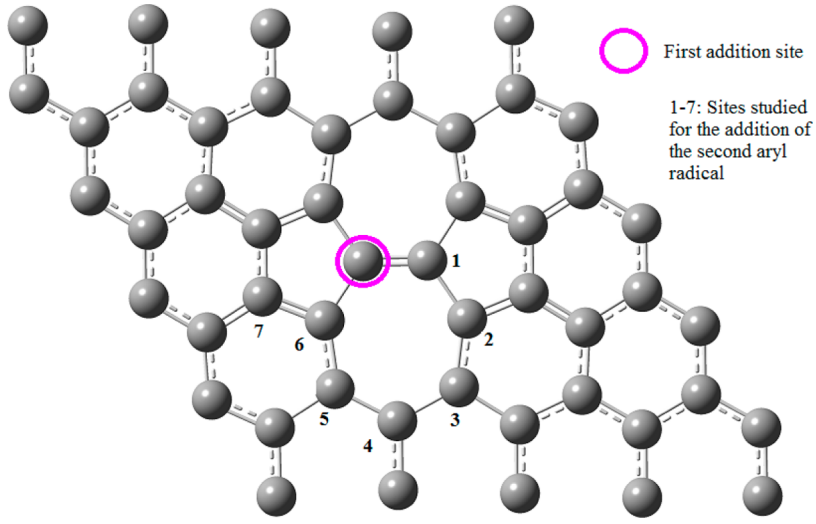


**Figure 8.** Addition sites studied for the addition of 2 aryl radicals onto Stone−Wales 5 × 5 graphene. Corresponding binding energies are presented in Table 4.

and one pentagon. The scenario for the single vacancy is slightly different. In this case, the nearby carbon atoms are not the most reactive ones. There is a strong preference for the addition onto carbon number 4 (numbering as in Figure 4), which is one of the atoms that were bonded to the missing carbon atoms. In contrast with the results obtained for the other defects, the addition of a second radical does not increase the reactivity of the defect. In this sense, the BE per aryl group is 71.3, nearly 30 kcal/mol smaller than the BE determined for the addition of one aryl group to the single vacancy.

## 4. CONCLUSIONS

By means of first-principle calculations, we have studied the reactivity of single vacancies, 585 double vacancies, 555−777 reconstructed double vacancies, Stone−Wales defects, and hydrogenated zigzag and armchair edges. The following are considered to be the most important findings of this work:

(1) The addition of H, F, and phenyl groups to defective graphene suggests the reactivity depends on the type and number of functional groups attached. For the addition of one functional group, we observed the following order of decreasing reactivity: single vancancy > hydrogenated zigzag edge > 585 double vacancy > 555−777 reconstructed double vacancy > Stone−Wales > hydrogenated armchair edge > perfect graphene. However, when two phenyl groups are attached, the Stone−Wales defect becomes more reactive than the 585 double vacancy and 555−777 reconstructed double vacancy.

(2) The extent to which defects increase reactivity is strongly dependent on the functional group attached to the structure. The lower the binding energy of the functional group onto perfect graphene, the larger the increase in reactivity.

(3) The reactivity of edges as compared with perfect graphene is much higher than the observed experimental value. In the particular case of the aryl diazonium salt, the experiment suggested that the edges are at least two times more reactive than the basal plane of graphene. Our results indicate that the hydrogenated zigzag and armchair are 5.07 and 2.68 times more reactive than perfect graphene


dx.doi.org/10.1021/jp4061945 | J. Phys. Chem. C 2013, 117, 19048−19055

**Table 4. Electronic Binding Energies (kcal/mol), for the Covalent Addition of Two Aryl Radicals $C_6H_4R$, onto Defective 5 × 5 Graphene Bearing Single Vancancy, Stone−Wales, and 555-777 Defect Sites**

| | SS singlet | OS singlet | SS triplet | OS triplet |
|---|---|---|---|---|
| Vac-1 | *a* | 49.4 | *a* | 51.7 |
| Vac-2 | 58.1 | 59.7 | 46.1 | 48.6 |
| Vac-3 | 52.1 | 57.9 | 49.2 | 51.9 |
| Vac-4 | 61.2 | 71.3 | 55.9 | 72.3 |
| Vac-5 | 51.6 | 55.4 | 48.2 | 51.9 |
| Vac-6 | 60.4 | 62.6 | 52.1 | 53.9 |
| Vac-7 | 51.12 | 50.2 | 65.1 | 45.0 |
| SW-1 | *a* | 52.2 | *a* | 22.8 |
| SW-2 | 32.2 | 35.2 | 23.1 | 27.3 |
| SW-3 | 33.1 | 30.6 | 24.6 | 21.7 |
| SW-4 | 33.9 | 28.4 | 27.9 | 22.4 |
| SW-5 | 29.9 | 25.4 | 24.8 | 20.5 |
| SW-6 | *a* | 34.1 | *a* | 29.7 |
| SW-7 | 29.4 | 29.4 | 24.6 | 24.5 |
| 555−777-1 | *a* | 44.4 | *a* | 36.2 |
| 555−777-2 | 22.5 | 30.3 | 28.5 | 23.9 |
| 555−777-3 | 29.1 | 34.2 | 26.6 | 22.8 |
| 555−777-4 | 31.9 | 37.1 | 29.7 | 29.7 |
| 555−777-5 | 34.9 | 41.8 | 28.9 | 31.6 |
| 555−777-6 | *a* | 40.8 | *a* | 35.6 |
| 555−777-7 | 22.0 | 32.3 | 26.9 | 27.3 |

[a]Not computed as it involves the addition in a nearby carbon atom, which causes the aryl groups to come too close.

**Table 5. Electronic Binding Energies (kcal/mol), for the Covalent Addition of Two Aryl Radicals $C_6H_4R$, onto Defective 5 × 5 Graphene Bearing a 585 Defect Site**

| | SS singlet | OS singlet | SS triplet | OS triplet |
|---|---|---|---|---|
| 585-1 | *a* | 47.3 | *a* | 36.3 |
| 585-2 | 26.2 | 31.6 | 21.7 | 28.8 |
| 585-3 | 41.9 | 46.5 | 30.0 | 33.5 |
| 585-4 | 37.3 | 37.8 | 30.1 | 32.9 |
| 585-5 | 41.5 | 40.0 | 30.3 | 28.9 |
| 585-6 | 37.7 | 36.3 | 33.9 | 31.4 |
| 585-7 | 43.1 | 44.0 | 33.0 | 33.5 |
| 585-8 | 36.5 | 33.8 | 29.7 | 27.3 |
| 585-9 | 32.4 | 34.7 | 25.3 | 26.9 |
| 585-10 | *a* | 48.7 | *a* | 43.3 |
| 585-11 | 35.5 | 38.5 | 28.8 | 32.0 |
| 585-12 | 35.8 | 32.9 | 33.7 | 31.7 |
| 585-13 | *a* | 44.4 | *a* | 36.8 |
| 585-14 | 40.2 | 37.0 | 33.1 | 27.7 |

[a]Not computed as it involves the addition in a nearby carbon atom, which causes the aryl groups to come too close.

(4) When two groups are attached onto a 585, 555−777, or Stones−Wales defect, they prefer to be paired on the same CC bond on opposite sides of the sheet. However, for the single vacancy, this is not the observed behavior as the preferred addition sites are those carbon atoms that were bonded to the missing carbon.

## AUTHOR INFORMATION


### Corresponding Author

*(P.A.D.) E-mail: pablod@fq.edu.uy. Tel: +59899714280. Fax: +589229241906.


### Notes

The authors declare no competing financial interest.

## ACKNOWLEDGMENTS

The author thanks PEDECIBA Quimica and ANII (FSE-6160) for financial support and Walter Shands from Intel corporation for his help with Intel cluster studio.

## REFERENCES


(1) Banhart, F.; Kotakoski, J.; Krasheninnikov, A. V. Structural Defects in Graphene. *ACS Nano* **2011**, *5*, 26−41.

(2) Dettori, R.; Cadelano, E.; Colombo, L. Elastic Fields and Moduli in Defected Graphene. *J. Phys.: Condens. Matter* **2012**, *24*, 104020.

(3) Ma, Y.; Lehtinen, P. O.; Foster, A. O.; Nieminen, R. M. Magnetic Properties of Vacancies in Graphene and Single-Walled Carbon Nanotubes. *New J. Phys.* **2004**, *6*, 68.

(4) Lehtinen, P. O.; Foster, A. S.; Ma, Y.; Krasheninnikov, A. V.; Nieminen, R. M. Irradiation-Induced Magnetism in Graphite: A Density Functional Study. *Phys. Rev. Lett.* **2004**, *93*, 187202.

(5) Denis, P. A.; Faccio, R.; Iribarne, F. How is the Stacking Interaction of Bilayer Graphene Affected by the Presence of Defects? *Comput. Theor. Chem.* **2012**, *995*, 1−7.

(6) Denis, P. A. Density Functional Investigation of Thioepoxidated and Thiolated Graphene. *J. Phys. Chem. C* **2009**, *113*, 5612−5619.

(7) Denis, P. A.; Iribarne, F. The 1,3 Dipolar Cycloaddition of Azomethine Ylides to Graphene, Single Wall Carbon Nanotubes, and $C_{60}$. *Int. J. Quantum Chem.* **2010**, *110*, 1764−1771.

(8) Al-Aqtash, N.; Vasiliev, I. Ab Initio Study of Carboxylated Graphene. *J. Phys. Chem. C* **2009**, *113*, 12970−12975.

(9) Ghaderi, N.; Peressi, M. First-Principle Study of Hydroxyl Functional Groups on Pristine, Defected Graphene, and Graphene Epoxide. *J. Phys. Chem. C* **2010**, *114*, 21625−21630.

(10) Cabrera-Sanfelix, P.; Darling, G. R. Dissociative Adsorption of Water at Vacancy Defects in Graphite. *J. Phys. Chem. C* **2007**, *111*, 18258−18263.

(11) Malola, S.; Hakkinen, H.; Koskinen, P. Gold in Graphene: In-Plane Adsorption and Diffusion. *Appl. Phys. Lett.* **2009**, *94*, 043106.

(12) Logsdail, A. J.; Akola, J. Interaction of $Au_{16}$ Nanocluster with Defects in Supporting Graphite: A Density-Functional Study. *J. Phys. Chem. C* **2011**, *115*, 15240−15250.

(13) Lim, D.-H.; Suarez Negreira, A.; Wilcox, J. DFT Studies on the Interaction of Defective Graphene-Supported Fe and Al Nanoparticles. *J. Phys. Chem. C* **2011**, *115*, 8961−8970.

(14) Lim, D.-H.; Wilcox, J. DFT-Based Study on Oxygen Adsorption on Defective Graphene-Supported Pt Nanoparticles. *J. Phys. Chem. C* **2011**, *115*, 22742−22747.

(15) Lim, D.-H.; Wilcox, J. Mechanisms of the Oxygen Reduction Reaction on Defective Graphene-Supported Pt Nanoparticles from First-Principles. *J. Phys. Chem. C* **2011**, *116*, 3653−3660.

(16) Liu, Y.; Wilcox, J. $CO_2$ Adsorption on Carbon Models of Organic Constituents of Gas Shale and Coal. *Environ. Sci. Technol.* **2011**, *45*, 809−814.

(17) Liu, Y.; Wilcox, J. Effects of Surface Heterogeneity on the Adsorption of $CO_2$ in Microporous Carbons. *Environ. Sci. Technol.* **2012**, *46*, 1940−1947.

(18) Liu, Y.; Wilcox, J. Molecular Simulation Studies of $CO_2$ Adsorption by Carbon Model Compounds for Carbon Capture and Sequestration Applications. *Environ. Sci. Technol.* **2013**, *47*, 95−101.

(19) Meyer, J. C.; Kisielowski, C.; Erni, R.; Rossell, M. D.; Crommie, M. F.; Zettl, A. Direct Imaging of Lattice Atoms and Topological Defects in Graphene Membranes. *Nano Lett.* **2008**, *8*, 3582−3586.

(20) Ugeda, M. M.; Brihuega, I.; Hiebel, F.; Mallet, P.; Veuillen, J.; Gomez-Rodriguez, J. M.; Yndurain, F. Electronic and Structural Characterization of Divacancies in Irradiated Graphene. *Phys. Rev. B* **2012**, *85*, 121402R.

(21) Dai, J.; Yuan, J.; Giannozzi, P. Gas Adsorption on Graphene Doped With B, N, Al, and S: A Theoretical Study. *Appl. Phys. Lett.* **2009**, *95*, 232105.

(22) Dai, J.; Yuan, J. Modulating the Electronic and Magnetic Structures of P-Doped Graphene by Molecule Doping. *J. Phys.: Condens. Matter* **2010**, *22*, 225501.
(23) Denis, P. A.; Faccio, R.; Mombru, A. W. Is It Possible to Dope Single-Walled Carbon Nanotubes and Graphene with Sulfur? *ChemPhysChem* **2009**, *10*, 715−722.
(24) Denis, P. A.; Iribarne, F. On the Hydrogen Addition to Graphene. *J. Mol. Struct.* **2009**, *907*, 93−103.
(25) Denis, P. A.; Iribarne, F. Thiophene Adsorption on Single Wall Carbon Nanotubes and Graphene. *J. Mol. Struct.* **2010**, *957*, 114−119.
(26) Deng, X.; Wu, Y.; Dai, J.; Kang, D.; Zhang, D. Electronic Structure Tuning and Band Gap Opening of Graphene by Hole/Electron Codoping. *Phys. Lett.* **2011**, *375*, 3890−3894.
(27) Zou, Y.; Li, F.; Zhu, Z. H.; Zhao, M. W.; Xu, X. G.; Su, X. Y. An Ab Initio Study on Gas Sensing Properties of Graphene and Si-Doped Graphene. *Eur. Phys. J. B* **2011**, *81*, 475−479.
(28) Denis, P. A. Band Gap Opening of Monolayer and Bilayer Graphene Doped With Aluminium, Silicon, Phosphorus, and Sulphur. *Chem. Phys. Lett.* **2010**, *492*, 251−257.
(29) Denis, P. A. When Noncovalent Interactions Are Stronger than Covalent Bonds: Bilayer Graphene Doped With Second Row Atoms, Aluminum, Silicon, Phosphorus and Sulphur. *Chem. Phys. Lett.* **2011**, *508*, 95−101.
(30) Suggs, K.; Reuven, D.; Wang, X. -Q. Electronic Properties of Cycloaddition-Functionalized Graphene. *J. Phys. Chem. C* **2011**, *115*, 3313−3317.
(31) Denis, P. A.; Iribarne, F. Monolayer and Bilayer Graphene Functionalized with Nitrene Radicals. *J. Phys. Chem. C* **2011**, *115*, 195−203.
(32) Denis, P. A. Chemical Reactivity of Lithium Doped Monolayer and Bilayer Graphene. *J. Phys. Chem. C* **2011**, *115*, 13392−13398.
(33) Wang, F. T.; Chen, L.; Tian, C. J.; Meng, Y.; Wang, Z. G.; Zhang, R. Q.; Jin, M. X.; Zhang, P.; Ding, D. J. Interactions Between Free Radicals and a Graphene Fragment: Physical Versus Chemical Bonding, Charge Transfer, and Deformation. *J. Comput. Chem.* **2011**, *32*, 3264−3268.
(34) Faccio, R.; Pardo, H.; Denis, P. A.; Yoshikawa Oreiras, R.; Araujo-Moreira, F. M.; Verissimo-Alves, M.; Mombru, A. W. Induced Magnetism by Single Carbon Vacancies in a 3-D Graphitic Network: a Supercell Study. *Phys. Rev. B* **2008**, *77*, 035416.
(35) Zhao, Y.; Truhlar, D. G. The M06 Suite of Density Functionals for Main group Thermochemistry, Thermochemical Kinetics, Noncovalent Interactions, Excited States, and Transition Elements: Two New Functionals and Systematic Testing of four M06-Class Functionals and 12 Other Functionals. *Theor. Chem. Acc.* **2008**, *120*, 215−241.
(36) Dion, M.; Rydberg, H.; Schroder, E.; Langreth, D. C.; Lundqvist, B. I. Van der Waals Density Functional for General Geometries. *Phys. Rev. Lett.* **2004**, *92*, 246401.
(37) Frisch, M. J.; Trucks, G. W.; Schlegel, H. B.; Scuseria, G. E.; Robb, M. A.; Cheeseman, J. R.; Scalmani, G.; Barone, V.; Mennucci, B.; Petersson, G. A.; et al. *Gaussian 09*; Gaussian, Inc.: Wallingford, CT, 2009.
(38) Soler, J. M.; Artacho, E.; Gale, J. D.; Garcia, A.; Junquera, J.; Ordejon, P.; Sanchez-Portal, D. The SIESTA Method for ab Initio Order-N Materials Simulation. *J. Phys.: Condens. Matter* **2002**, *14*, 2745−2779.
(39) Ordejon, P.; Artacho, E.; Soler, J. M. Self-Consistent Order-N Density-Functional Calculations for Very Large Systems. *Phys. Rev. B* **1996**, *53*, R10441−R10444.
(40) Boys, F. S.; F. Bernardi, F. The Calculation of Small Molecular Interactions by the Differences of Separate Total Energies. *Mol. Phys.* **1970**, *19*, 553−566.
(41) Troullier, N.; Martins, J. L. Efficient Pseudopotentials for Plane-Wave Calculations. *Phys. Rev. B* **1991**, *43*, 1993−2006.
(42) Hehre, W.; Radom, L.; Schleyer, P. v. R.; Pople, J. A. Ab Initio Molecular Orbital Theory; Wiley: New York,1986.
(43) Denis, P. A. Theoretical Investigation of the Stacking Interactions Between Curved Conjugated Systems and Their Interaction with Fullerenes. *Chem. Phys. Lett.* **2011**, *516*, 82−87.
(44) Sharma, S.; Kaik, J. H.; Perera, C. J.; Strano, M. S. Anomausly Large Reactivity of Single Graphene Layers and Edges Towards Electron Transfer Chemistries. *Nano Lett.* **2010**, *10*, 398−405.
(45) Denis, P. A.; Iribarne, F. Cooperative Behavior in Functionalized Graphene: Explaining the Occurrence of 1,3-Cycloaddition of Azomethine Ylides onto Graphene. *Chem. Phys. Lett.* **2013**, *550*, 111−117.
(46) Denis, P. A.; Iribarne, F. [2 + 2] Cycloadditions onto Graphene. *J. Mater. Chem.* **2012**, *22*, 5470−5477.